FABRICATION AND CHARACTERISATION OF NICKEL - METAL HYDRIDE BATTERY

A Thesis Submitted

in Partial Fulfillment of the Requirements

for the Degree of

Master of Technology

by

Sanjiv Tripathi

to the

MATERIALS SCIENCE PROGRAMME

INDIAN INSTITUTE OF TECHNOLOGY, KANPUR

December,1996

MSP-1996-M-TRI-FAB

CERTIFICATE

This is to certify that the work contained in the thesis entitled "*Fabrication and characterisation of nickel - metal hydride battery*" by Mr. Sanjiv Tripathi , has been carried out under our supervision and has not been submitted elsewhere for a degree.

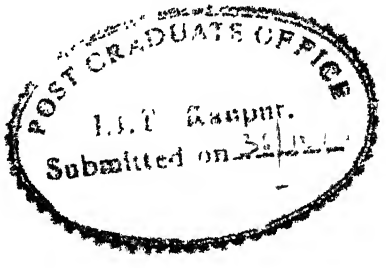

(K. N Rai)
Professor
Materials Science Programme
Indian Institute of Technology
Kanpur - 208 016

Jitendra Kumar
(Jitendra Kumar)
Professor
Materials Science Programme
Indian Institute of Technology
Kanpur - 208 016

December , 1996

Dedicated to

My Parents

Abstract

The demand of rechargeable batteries for portable applications is continuously increasing . Of the known batteries, nickel-cadmium has an impressive power rating . However, they have slow recharge rate and cadmium being a poisonous metal becomes an enviornmental hazard on disposal. The Lead-acid batteries ,being another option, have lesser energy storage capacity and smaller life as compared to Ni-Cd batteries. This has encouraged development of nickel-meatl hydride (Ni-MH) batteries having characteristics similar to that of Ni-Cd batteries and at the same time posing no enviornmental pollution . Their fabrication, however, involves intricate processes and is a matter of trade secret. An attempt has therefore been undertaken to fabricate Ni-MH rechargeable cylindrical batteries (size 'AA') by using $LaNi_5$ as active material with silicone sealant as binder for negative electrode , $Ni(OH)_2$ as positive electrode , 8.5 molal solution of KOH as an electrolyte and a combination of nylone cloth and glass wool as separator . Two types of negative electrodes have been fabricated, one using bare $LaNi_5$ and other with nickel coated $LaNi_5$ as an active material . The crystalline phases of electrodes have been identified by powder X-ray diffraction technique. The electrical characteristics of batteries are studied by discharging through a resistor of 920 ohm. The stability of both types of electrodes have been examined in terms the number of cycles and shelf storage.

The typical open circuit voltage is found to be 1 3 V and energy density 656

J-s/kg. Further, it is demonstrated that electrodes with nickel coated $LaNi_5$ provides better stability, lesser capacity loss and longer shelf life in nickel metal hydride batteries. It is believed that nickel coating prevents oxidation of the active material $LaNi_5$ and leads to improvement in the recycling capacity and the shelf life of the Ni-MH battery.

Acknowledgements

I express my gratitude to my supervisors Prof. K N Rai and Prof. Jitendra Kumar for providing me invaluable guidance , encouragement and spending a lot of time on small details during the course of investigation.

I am indebted to Dr. D. C Agrawal , Dr. K Shahi , Dr. Y N. Mohapatra and Dr. S. Kar for their interest .

I am thankful to Dr M. N. Mungole and Mr. Subhash Chand for providing me timely help all along.

Thanks are due to all my friends Vishnukant , R K Gupta , Giridhar Kumar , T. Ansari , J. Singh , Rajesh Kumar , Vipin Jain , A. S. Rajput , N. K. Puthal , Sangeet , Pragya , Avi Prakash, M. P. Agrawal, Akshat Agrawal, B. N. Srivastava , M. K. Singh , K. K. Lakhmani and many others for giving me full moral support and making my stay at I. I. T. , Kanpur memorable.

I acknowledge the support and cooperation secured from all the office and lab staffs of A. C. M. S. , I. I. T. , Kanpur.

Finally, I am thankful to my family members whose inspiration and moral support brought best out of me , culminating in this thesis.

Sanjiv Tripathi

List of Tables

List of Figures

Contents

Chapter 1

Introduction

The present chapter is devoted to basic understanding of a battery in terms of its components, electrochemical principles, thermodynamics and kinetics of the electrode processes involved.

1.1 General description of a battery

A cell is the basic building block of a battery and consists of three major components , the anode , the cathode , and the electrolyte. The anode or negative electrode is a reducing electrode and gives up electrons to the external circuit and is oxidized during electrochemical reaction. Thus, it must be an efficient reducing agent having good conductivity and stability The cathode or positive electrode is an oxidizing electrode which accepts electrons from external circuit and is reduced during electrochemical reaction. Clearly, it has to be an efficient oxidizing agent with good conductivity and stability. The electrolyte is an ionic conductor and provides medium for transfer of electric charge inside the cell between the anode and the cathode. It should have good ionic conductivity, poor reactivity with the electrode material, thermally stable and safe. A separator is usually inserted between the two

electrodes to physically separate them. It is permeable to electrolyte so as to allow the charge transfer [1-3].

The term battery is generally adopted to describe a single unit ready to use and comprised of one or more cells (connected in series or paralled) provided with terminals and proper insulation (Fig.1.1.). The batteries are classified as primary and secondary:

A primary battery can be used only once and discarded as its active materials are used up during reaction produc ing electrical energy . Its examples include Zn / C , Mg / MnO_2 , Zn / HgO , Zn / Ag_2O , etc. On the other hand, a secondary battery is made to use repeatedly by reversing the chemical reaction by passing the current and storing the energy in the process called recharging. These are also known as storage batteries or accumulators, e.g., Lead-acid, Ni - Cd , Ni - Fe , Ag - Cd ,etc. fall under this category [1-3].

1.2 The electrode potential

When a metal is immersed in an aqueous solution, it tends to pass into solution in the form of ions. This tendency is, however, opposed by dissolved ions, which try to deposit back on the metal surface. When these two forces become equal, equilibrium is attained. The value of equilibrium potential is called the electrode potential of the metal. When the ions leave, an equivalent number of electrons are accumulated on the surface of the metal. This process sets-up an electrostatic field which tries to hold the positive ions close to the metal surface. Thus, an electric double layer is formed. If the dissolved metal ions are removed from the solution, equilibrium is disturbed and more metal dissolves until equilibrium is attained afresh. The greater is the tendency of a metal to pass into the solution, larger

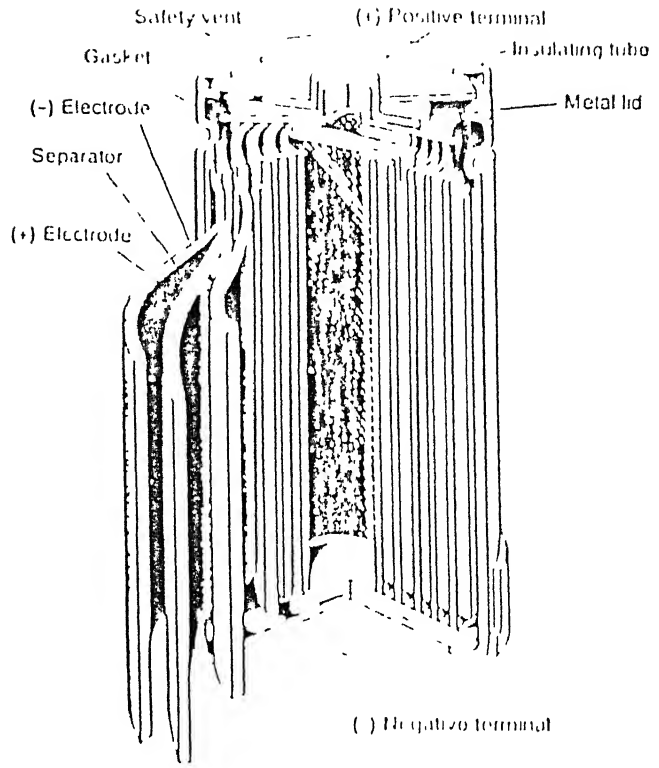

Figure 1.1 : Construction of a sealed cylindrical battery [

is the number of electrons accumulated on the metal surface making the electrode potential of the metal more negative [4-6] The electrode potential is determined in comparison to a standard electrode i.e. by the emf of a cell made of two electrodes .

The electrochemical potential ($\bar{\mu}$) for an ion is [4]:

$$\bar{\mu} = \mu + nF\,E \tag{1 1}$$

where μ is the chemical potential defined as free energy per mole of a substance, n is the number of electrons, F is the Faraday constant (96,500 coulombs), E is the electrode potential of the metal. So, the change in the electrochemical potential of an ion, taking part in an electrode process is given by

$$\Delta\bar{\mu} = \Delta\mu + nF \times \Delta E \tag{1.2}$$

Under dynamic equilibrium , the eletrochemical potential of the ions in metal and solution equilizes, such that

$$\Delta\bar{\mu} = 0 \tag{1.3}$$

This means that the chemical and the electrical potential differences counterbalance each other and no net transfer of ions takes place. Eq. (1.2) then gives

$$\Delta\mu = -nF \times \Delta E \tag{1.4}$$

or

$$\Delta G = -nF \times \Delta E \tag{1.5}$$

where ΔG is the free energy change occurring in the electrode reaction and ΔE is the electrode potential with respect to a reference electrode. Under standard conditions (i.e., pure metal with its activity in solution being unity), we write [4]

$$\Delta G^\circ = -nF\Delta E^\circ \tag{1.6}$$

Thus, the change in the electrode potential can be calculated from free energy data or measured experimentally.

When two electrodes are immersed in an electrolyte, each develops a potential of its own. Their difference then characterises the cell potential In a battery electrochemical reaction includes oxidation and reduction of the active material on the anode and cathode,respectively. For example, in a Ni - Cd battery, the reactions are [2]

$$2Ni(OH)_2 + 2OH^- \underset{discharge}{\overset{charge}{\rightleftharpoons}} 2NiOOH + 2H_2O + 2e^- \qquad \Delta E^\circ = -0.49\ volt \tag{1.7}$$

$$Cd(OH)_2 + 2e^- \underset{discharge}{\overset{charge}{\rightleftharpoons}} Cd + 2OH^- \qquad \Delta E^\circ = +0.81\ volt \tag{1 8}$$

and the cell potential under standard conditions becomes -0 49 - (+0.81) = -1.30 V

1.3 Thermodynamic background

For a hypothetical cell reaction

$$a.A + b.B \rightleftharpoons c.C + d.D \tag{1.9}$$

where A and B are reactants, C and D are products and a,b,c,d some numbers, the Gibb's free energy change (ΔG) at equilibrium is given by [2]

$$\Delta G = RT\ ln\frac{[C]^c[D]^d}{[A]^a[B]^b} \tag{1.10}$$

where [A] represents the activity or molar concentration. The voltage ΔE of a cell is given by

$$\Delta E = \Delta E^\circ - \frac{RT}{nF}\ ln\frac{[C]^c[D]^d}{[A]^a[B]^b} \tag{1.11}$$

When a cell is discharged the energy flows through the conducting wires. A part of this energy appears as heat (ΔQ) It amounts to an irreversible process. The change in the entropy (ΔS) at temperature T associated with heat effect is given by [2]

$$\Delta S = \frac{(\Delta Q)_R}{T} \tag{1.12}$$

or

$$\Delta S = n.F.(\frac{\partial E}{\partial T}) \tag{1.13}$$

where $(\frac{\partial E}{\partial T})$ is the temperature coefficient of EMF of a reversible cell. The enthalpy ($\Delta H = \Delta G + T\Delta S$) of reaction is given by

$$\Delta H = -n.F.\Delta E + n.F.T(\frac{\partial E}{\partial T})_P \tag{1.14}$$

This is the Gibbs-Helmholtz equation in electrical units.

The ratio ($\epsilon = \frac{\Delta G}{\Delta H}$) of Gibb's free energy change and enthalpy change gives the thermodynamic efficiency of the system [2]. Thus, combining (1.5) and (1.14), we have

$$\epsilon = 1 + \frac{n.F.T}{\Delta H}(\frac{\partial E}{\partial T})_P \tag{1 15}$$

It is clear that the efficiency increases with increase in temperature for systems having a positive temperature coefficient $(\frac{\partial E}{\partial T})_P$ But, for Ni-Cd system, temperature coefficient is negative. So, its thermodynamic efficiency decreases with increase in

temperature. The enthalpy change involve is 33 kilocalorie per equivalent weight and thermodynamic efficiency is 0.89 at 25°C.

1.4 Kinetics of electrode processes

When a current is passed through an electrochemical cell, the process which opposes the flow and responsible for lowering of the cell potential from its equilibrium value is called polarization. Three main polarizations are described below .

1.4.1 Concentration polarization

Let us consider a metal rod M dipped in a solution containing M^+ ions. The electrode develops a certain potential(ΔE_1) depending upon its tendency to release ions and their cocentration in the solution itself.

$$M \rightarrow M^{+n} + ne^- \tag{1.16}$$

If metal is made the cathode and the potential is applied, the metal ions will begin to be discharged and there will be a fall in the ion concentration in the vicinity of the metal electrode. If the fall is not made up by the immediate migration of the M^+ ions from the solution to cathode surface, the changes in electrode potential are given by the Nerst equation as

$$\Delta E_2 = \Delta E^\circ + \frac{RT}{nF}\, ln[a_M^{+n}] \tag{1.17}$$

and

$$\Delta E_1 = \Delta E^\circ + \frac{RT}{nF}\, ln[a_S^{+n}] \tag{1.18}$$

such that

$$\Delta E_2 - \Delta E_1 = \frac{RT}{nF} \ln \frac{[a_M^{+n}]}{[a_S^{+n}]} \tag{1.19}$$

This phenomenon of departure of the electrode potential from the equilibrium value as a result of the change of concentration in the vicinity of the electrode is known as concentration polarization [4,5].

1.4.2 Activation polarization

It occurs due to sluggish electrode reaction or in other words when an activation energy is required to overcoming the reaction hindrance. If a metal is submerged in solution containing its own ions , a dynamic equilibrium is established, as much metal being dissolved as is redeposited in the same time. Such an ion transport through the phase boundary is referred to as exchange current density and is denoted by i_0. If the electrode is made an anode in an electrolyte bath with a resulting net dissolution of metal, the cathodic partial current (i_c) is decreased while anodic partial current (i_a) increases. The impressed net current is

$$I_a = i_a - i_c \tag{1.20}$$

By connecting the metal as a cathode, we find correspondingly

$$I_c = i_c - i_a \tag{1.21}$$

The equilibrium between a non - corroding metal and a solution containing its ions corresponds to the point $\frac{E_0}{i_0}$ in the polarization diagram (Fig. 1.2), where E_0 is the reversible equilibrium potential of the metal in the solution and i_0 is the exchange current. By examining the derivation of the electrode potential of the metal from the equilibrium value E_0 by anodic current I_a, one obtains [1] :

1. For small value of I_a ($< 10\ i_0$), overpotential varies linearly with I_a, such that

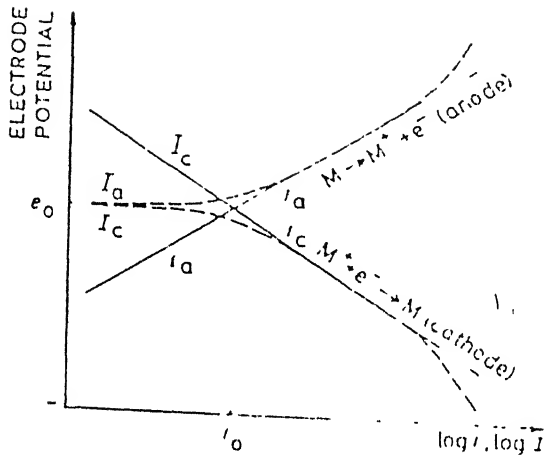

Figure 1 2: Polarization conditions of a non-corroding electrode

$$\eta_a = \frac{RT}{z.F} \times \frac{I_a}{i_o} \tag{1.22}$$

In a half-logarithmic diagram, this corresponds to a dashed curve shown in Fig. 1.2

2. For $I_a > 10\ i_0$, overpotential η_a is given by Tafel's equation

$$\eta_a = b.\ ln\frac{I_a}{i_0} = a + b\ lnI_a \tag{1.23}$$

where a and b ($= \frac{2RT}{F}$) are constants In the half logarithmic diagram, one then obtains Tafel straight lines

3. For I_a much greater than i_0, polarization occurs again because of cocentration gradient and/or resistance manifesting derivations from the Tafel lines (Fig. 1.2).

1.4.3 Ohmic polarization

It is defined as cell internal impedance loss. It is proportional to current drawn from the system and commonly termed as ohmic polarization [1]. It depends upon (a) resistance of electrolyte and current collector, and (b) contact resistance between active mass and the current collector. The cell voltage ΔE can be expressed as

$$\Delta E = \Delta E_o - [(\eta_{ct})_a + (\eta_c)_a] - [(\eta_{ct})_c + (\eta_c)_c] - iR_i \tag{1.24}$$

where ΔE_0 is the open circuit voltage of the cell, $(\eta_{ct})_a$ and $(\eta_{ct})_c$ are the activation polarization or charge transfer overvoltage of cathode and anode, $(\eta_c)_a and (\eta_c)_c$ are the concentration polarization of anode and cathode, i is the operation current

of cell on load, and R_i is the internal resistance of the cell. The ohmic polarisation disappears in a few microseconds after the current is stopped

In battrey design, one tries to ensure minimum energy losses. Some factors which help in achieving this objective are as follows :

1. high conductivity of the electrolyte reduces ohmic polarization.
2. high chemical stability of electrolyte avoids reaction with electrodes.
3. use of porous electrodes provides high surface area within a given geometric dimension and keeps activation polarization to a bare minimum.
4. a proper cell design facilitates easy mass transfer (or diffusion) of the reaction products from the electrode surface through the electrolyte and, in turn, reduces the cocentration polarization.
5. a current collector characterized by high corrosion resistance provides uniform current distribution and low contact resistance and minimises the ohmic polarization.

Chapter 2

The nickel - metal hydride battery

Hydrogen has an extremely high energy density per unit weight (The energy density for Nickel-hydrogen battery is 55 Wh/kg as compared to 35 Wh/kg for Lead acid battery). This property has led to develop systems which can use hydrogen as a fuel [7,8]. One of the greatest limitations in the usage of hydrogen is , however, caused by the difficulty encountered in its economic and convenient storage. The most common method being as gaseous cylinders at high pressure. This is most safe but the amount of hydrogen stored is low. Alternatively, hydrogen can be collected in a dewar after liquidification at $-240°C$, which is a very expensive proposition. Fortunately, hydrogen reacts with certain metals and intermetallics (e.g., Pd, $LaNi_5$, $SmCo_5$, FeTi, Mg_2Ni, etc.) and forms hydride sponges. The density of hydrogen thus stored is more than that of liquid hydrogen and can be released at convenient temperature and pressure at will [9].These properties led to the development of metal hydride electrodes for rechargeable batteries [10]. In fact, metal hydride electrode replaces the toxic cadmium electrode used in Ni-Cd alkaline batteries and offers several advantages, viz., (a) high energy density so less active materials, (b) cadmium

free environment resulting in lesser disposal problems, (c) maintenance free because of sealed construction, (d) long self life, (e) rapid recharging capability, etc..

2.1 Basic reactions

In nickel-metal hydride (Ni-MH) battery, the positive electrode is made of $Ni(OH)_2$ while the negative electrode is of a metal or intermetallic, having capacity to store hydrogen as hydride [7]. Both the electrodes have a separator in between for electrical insulation All these are dipped in an electrolyte (say, aq. KOH). A schematic diagram of Ni-MH battery is shown in Fig. 2.1. The reactions during charging and discharging processes are represented as

$$Ni(OH)_2 + OH^- \underset{discharging}{\overset{charging}{\rightleftharpoons}} NiOOH + H_2O + e^- \tag{2.1}$$

$$M + H_2O + e^- \underset{discharging}{\overset{charging}{\rightleftharpoons}} MH + OH^- \tag{2.2}$$

The overall reaction is thus written by combining (2.1) and (2.2) as

$$Ni(OH)_2 + M \underset{discharging}{\overset{charging}{\rightleftharpoons}} NiOOH + MH \tag{2.3}$$

where M stands for the hydrogen absorbing alloy / intermetallic (say $LaNi_5$). Thus, during charging divalent Ni^{+2} oxidise to Ni^{+3} and H_2O disociates to give hydrogen atoms, which are absorbed by hydride forming metal / alloy / compound(M). During discharging, a reverse reaction takes place, i.e.. NiOOH converts back into $Ni(OH)_2$ and hydrogen atom from metal hydride is oxidised to H_2O. Here, OH^- ions consumed at the positive electrode are equal to OH^- produced at the negative electrode and hence no consumption of electrolyte takes place. As the equilibrium electrode

free environment resulting in lesser disposal problems, (c) maintenance free because of sealed construction, (d) long self life, (e) rapid recharging capability, etc .

2.1 Basic reactions

In nickel-metal hydride (Ni-MH) battery, the positive electrode is made of $Ni(OH)_2$ while the negative electrode is of a metal or intermetallic, having capacity to store hydrogen as hydride [7]. Both the electrodes have a separator in between for electrical insulation. All these are dipped in an electrolyte (say, aq. KOH). A schematic diagram of Ni-MH battery is shown in Fig. 2.1. The reactions during charging and discharging processes are represented as

$$Ni(OH)_2 + OH^- \underset{discharging}{\overset{charging}{\rightleftharpoons}} NiOOH + H_2O + e^- \tag{2.1}$$

$$M + H_2O + e^- \underset{discharging}{\overset{charging}{\rightleftharpoons}} MH + OH^- \tag{2.2}$$

The overall reaction is thus written by combining (2.1) and (2.2) as

$$Ni(OH)_2 + M \underset{discharging}{\overset{charging}{\rightleftharpoons}} NiOOH + MH \tag{2.3}$$

where M stands for the hydrogen absorbing alloy / intermetallic (say $LaNi_5$). Thus, during charging divalent Ni^{+2} oxidise to Ni^{+3} and H_2O disociates to give hydrogen atoms, which are absorbed by hydride forming metal / alloy / compound(M). During discharging, a reverse reaction takes place, i.e.. NiOOH converts back into $Ni(OH)_2$ and hydrogen atom from metal hydride is oxidised to H_2O. Here, OH^- ions consumed at the positive electrode are equal to OH^- produced at the negative electrode and hence no consumption of electrolyte takes place. As the equilibrium electrode

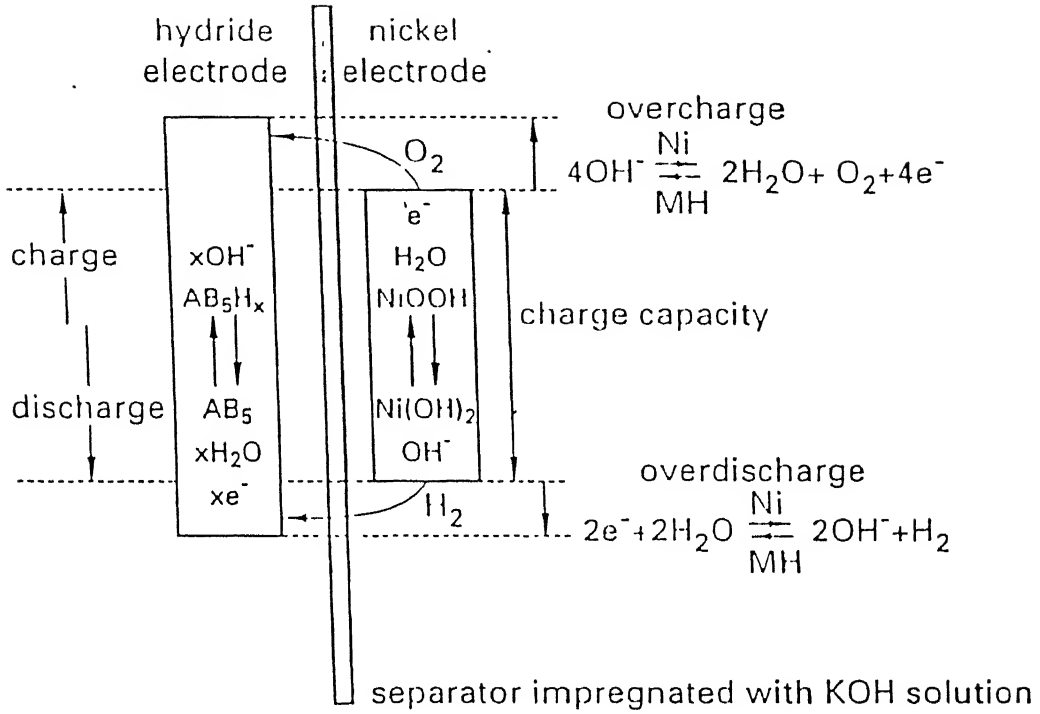

Figure 2.1 : Schematic representation of the concept of sealed rechargable nicke metal hydride (Ni-MH) battery [1]

potential of nickel electrode is + 439mV and that of $LaNi_5$ is -861mV, the open circuit potential of Ni-MH battery is just the difference of the two, i.e., 1.3V.

2.2 Side reactions

In Ni-MH batteries, some side reactions also occur at the electrodes, e.g., oxidation of hydroxyl (OH^-) ions with simultaneous evolution of oxygen at nickel electrode and reduction at the MH electrode [7] :

$$4OH^- \xrightarrow{Ni} O_2 + 2H_2O + 4e^- \tag{2.4}$$

$$O_2 + 2H_2O + 4e^- \xrightarrow{MH} 4OH^- \tag{2.5}$$

As a consequence, the partial pressure of oxygen inside the battery increases. But, oxygen passes through the electrolyte in the meantime and reaches MH electrode, where it forms OH^- ions by converting the metal hydride back into a metal. Obviously, the partial pressure of oxygen inside the battery is in general very low. Under steady state conditions, amounts of oxygen evolved at the Ni electrode and consumed at MH electrode are just equal [7] .

The above reactions become important when the battery approaches 75-80% of charge. As the oxygen recombination reaction is exothermic in nature, the temperature begins to rise rapidly at this stage and voltage passes through a maximum as battery reaches a full charge. Beyond this point, voltage drops, battery goes into overcharge but temperature continues to rise as all electrical energy supplied is then converted into heat. The amount of heat generated (Q) inside a battery is given by [11]

$$Q = i[-\frac{T.\,\Delta S}{nF} + \sum |\eta| + iR_i] \tag{2.6}$$

where i is the charging current, T is the temperature, n is the no. of electrons involved in the reaction, F is the Faraday constant, ΔS is the change in entropy, $\sum|\eta|$ represents various overpotential components, and R_i is the internal resistance of the battery. The effect of overpotential components becomes significant when oxygen recombination cycle starts at MH electrode and heat evolved increases sharply. Also, the overpotential for oxygen recombination is extremely high ($> 1V$). Thus, temperature rise can adversly affect the electrode properties and hence is avoided.

Similarly the reactions occurring at Ni electrode during discharge cycle are

$$2H_2O + 2e^- \xrightarrow{Ni} 2OH^- + H_2 \tag{2.7}$$

and results in pressure buildup inside the battery. As the affinity of MH electrode is excellent for hydrogen the following reaction takes place there

$$H_2 + 2OH^- \xrightarrow{MH} 2H_2O + 2e^- \tag{2.8}$$

MH electrode should, therefore, possess excellent physical properties so as to remain stable during discharging . The battery voltage is usually very close to zero specially under overdischarging condition.

2.3 Self discharging

The Ni-MH batteries lose their stored charge under open circuit conditions. This is termed as self discharge. Typically, self discharge rates at room temperature are 1-2% of the storage capacity per day. There are two mechanisms responsible for self-discharge:

(i)The reaction that occur at nickel electrode is

$$2NiOOH + 2OH^- \longrightarrow 2Ni(OH)_2 + O_2 + 2e^- \tag{2.9}$$

The electrons released by OH^- ions are accumulated at the Ni-electrode / electrolyte interface. However, the kinetics of the process is such that it takes quite a while before oxygen evolution becomes appreciable leading to capacity loss under self discharge Subsequently, the oxygen on reaching the MH electrode produces OH^- ions at the expense of charge stored there The reactions taking place are

$$O_2 + 2H_2O + 4e^- \xrightarrow{MH} 4OH^- \tag{2.10}$$

$$MH + OH^- \longrightarrow M + H_2O + e^- \tag{2.11}$$

Thus, the oxygen evolution at Ni electrode and recombination at MH electrode makes a gas phase shunt for the charge stored at electrodes.

ii) The hydrogen is also released at the MH electrode,

$$MH \longrightarrow M + \frac{1}{2}H_2 \tag{2.12}$$

This hydrogen on coming in contact with Ni electrode gets oxidised while the Ni electrode is simultaneously reduced according to the reactions

$$H_2 + 2OH^- \xrightarrow{Ni} 2H_2O + 2e^- \tag{2.13}$$

$$NiOOH + H_2O + e^- \longrightarrow Ni(OH)_2 + OH^- \tag{2.14}$$

Clearly, if partial pressure of hydrogen is high, more selfdischarge takes place. Obviously, discharging also occurs via hydrogen gas phase shunt between MH and Ni-electrodes [7].

2.4 The metal hydride electrode

If we look at the hydrogen and hydroxyl ion movements inside a battery, similarity between electrochemical charge transfer and hydride formation/ decomposition reaction via gas phase becomes obvious [7,12].

The hydride formation during reduction (or charging) involves (a) the supply of reactants by means of diffusion from the electrolyte to the solid / solution interface [5]. (b) charge transfer reaction leading to the formation of hydrogen and OH^- ions at the interface, (c) separation of reaction products, hydride formation through diffusion and transport of OH^- ions into the bulk of the electrolyte, and (d) evolution of H_2 from the electrode surface by process of recombination of adsorbed hydrogen species. These steps can be represented by the following reactions :

$$H_2O_{(bulk)} \longrightarrow H_2O_{(S)} \tag{2.15}$$

$$M + H_2O_{(S)} + e^- \longrightarrow MH_{(ads)} + OH^-_{(S)} \tag{2.16}$$

$$M H_{(ads)} \longrightarrow M H_{(hydride)} \tag{2.17}$$

$$OH^-_{(S)} \longrightarrow OH^-_{(bulk)} \tag{2.18}$$

$$2H_{(ads)} \longrightarrow H_2 \tag{2.19}$$

The reverse reaction sequence occurs during the oxidation (discharging) cycle.

In case of gas phase, hydrogen molecules come into contact with a hydride forming compound and get dissociated at the solid-gas interface. Atomic hydrogen

thus produced is adsorbed at the metal surface, which jumps into the interstitial site underneath, dissolves in the intermetallic and eventually forms the hydride exothermically [10]. In the reverse cycle, metal hydride dissociates by raising the temperature slightly and the hydrogen atoms diffuse to the surface where they recombine to form molecules and get liberated.

The equilibrium potential of metal hydride electrode at a temperature (T) is given by [7]

$$E_0 = -\frac{RT}{nF} \ln p_{H_2} \tag{2.20}$$

where p_{H_2} represents the equilibrium (plateau) pressure for adsorption and desorption of hydrogen, R is the gas constant, and n is the number of electrons involved in the reaction Thus, measurement of the equilibrium potential E_0 against a reference electrode can be used to determine the plateau pressure of the reaction [13]. Usually, electrode materials having characteristic hydrogen plateau pressure of 0.1-1 bar (i.e., 10^4 - 10^5 Pa) are desirable for Ni-MH batteries.

2.5 The nickel oxide electrode

Starting with metallic nickel, the α-$Ni(OH)_2$ is first prepared. This upon cycling and/or aging is converted to dehydrated β-$Ni(OH)_2$ and in turn to β-NiOOH. On further oxidation, β-NiOOH is transformed into γ-NiOOH which gets electrochemically reduced to α-$Ni(OH)_2$ (see, e.g., Fig. 2.2). The two β-modifications are identified as active materials in the Ni-electrode. Both these compounds exhibit brucite C6 hexagonal crystal structure (Fig. 2.3). The β-NiOOH is considered as H-deficient form of $Ni(OH)_2$. The precipitated form of these compounds contain small amount of H_2O and improves their electrical conductivity. Both the hydrated forms (i.e., α-$Ni(OH)_2$ and α-NiOOH) also crystalize in layered brucite structure

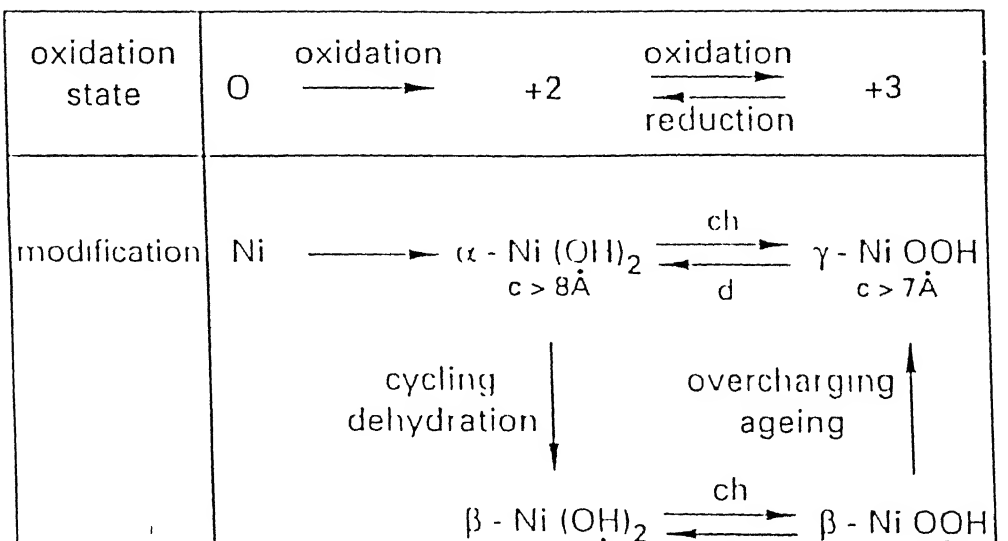

Figure 2.2 : Reaction scheme for the nickel electrode in alkaline solution [7]

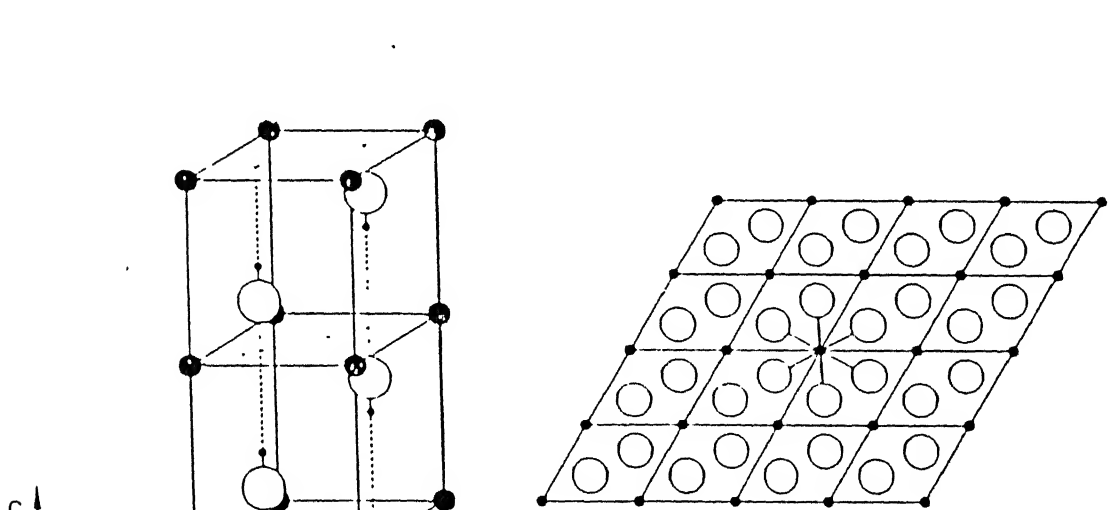

igure 2.3 : (a) Hexagonal crystal structure of β-Ni$(OH)_2$ and (b) Its projection on the basal plane (several unit-cells). The hydrogen atoms are omitted in (b) [7]

and contain intercalation layers of H_2O between Ni layers. As a result, c-axis is considerably increased. The presence of water layers enables easy ionic transport and is responsible for their improved electrical conductivity [7].

2.6 Present state of development

The fabrication of a battery electrode is very intricate process and a matter of trade secret. Most of the processes are patented with meagre details available. Some of the known processes for fabrication of electrodes related to nickel-metal hydride batteries are described below :

(a) Fabrication of nickel electrode: As described earlier, the nickel electrode consists of a nickel substrate (plate / grid / plaque) impregnated with $Ni(OH)_2$ on the surface. Conventionally, the Ni electrode is fabricated by sintering nickel powder in reduced atmosphere, and then impregnating electrochemically the active material $Ni(OH)_2$ into the pores [14,15]. In preparation of nickel plaque by sintering , nickel powder has been replaced by nickel fibres (20 μm dia) successfully [16]. Also, the decay in electrode capacity can be reduced if we add some cobalt together with $Ni(OH)_2$ [16].

A new technology has been developed by Varta Batteries Ltd., Germany, in which, PTFE powder along with a catalyst is mixed with nickel powder (grain size 30-40 μm) in a mill with fast rotating knives. This PTFE mixture is rolled in the form of a continuous tape, which is laid onto a wire grid for mechanical stability and current collection [20]. In yet another method, $Ni(OH)_2$ is mixed with a suitable binder (1 % carboximethyl cellulose) and mechanically pressed to obtain a nickel electrode [11].

(b) Hydride forming materials: The alloys / intermetallics used for fabricating a metal hydride (or anode) electrode may be grouped under different categories, viz AB_5, AB_2, and AB types [1]. $LaNi_5$ forms the basis of AB_5 type intermetallics and are usually prepared by arc-melting The choice lies on the hydrogen capacity and suitable metal-hydride bond strength. Lanthanum is replaced by mischmetal to reduce the cost. It is an anode material. Also, various modifications are introduced to improve the characteristics of $LaNi_5$ type system, e.g., the partial substitution of Ni with Ce, Sn, and Co results in expansion of the unit cell and lowers the hydrogen adsoption / desorption plateau pressure Also, the presence of Sn enhances the hydrogen storage capacity. These substitutions together with partial replacement of La with Ce leads to alloys having a general formula $La_{1-x}Ce_xNi_{5-y-z}Co_ySn_z$ and shown to retain high hydrogen storage capacity with longer cycle life [18]. The substitution of La and Ni by small amount of Zr and Al respectively have been found to improve the cycle life of $LaNi_5$ [19]. The multicomponent $La_{1-x}Ce_xNi_{3.35}Mn_{0.4}Al_{0.3}$ alloy is found to exhibit increasing corrosion resistance with increasing amount of Ce content [20]. The mischmetal based system appears to find extensive use in metal hydride batteries $MmNi_{3.5}Al_{0.7}Co_{0.8}$ (Mm → mischmetal with 24.8% La, 52.56% Ce, 5.57% Pr, 16.86% Nd and 0.14% Sm) improves the hydrogen absorption capacity when mixed with Co_3O_4 or RuO_2 [21]. Also, $MmNi_{3.5}Al_{0.7}Co_{0.8}$ on subjecting to mechanically grinding with cobalt metal powder for one hour shows higher discharge capacity and longer cycle life [22].

AB_2-type intermetallics consist of Mg_2Ni, Mg_2Cu and alloys of vanadium-titanium-zirconium-nickel. The electrodes fabricated using V-Ti-Zr-Ni exhibit improved energy density than $LaNi_5$ [1] The examples for AB-type intermetallics are FeTi, $Fe_{1-x}Mn_xTi$ and $Fe_{1-x}Ni_xTi$ [6]. An electrode fabricated using melt-extracted

fibres of $Ni_{64}Zr_{36}$ has recently been found to have high hydrogen storage capacity and low self discharge rate [23].

(c) **The MH electrode fabrication methods:** The metal hydride electrodes are fabricated by mechanically pressing (pressure $\approx$ 20.7 MPa) the well-mixed powders of the intermetallic compounds and an additive (in 1:1 ratio) on to a nickel (current collector) mesh at room temperature [24]. The additive (a binder) is carbon (Vulcan-XC-72, Norit-NIC or acetelene black XC-35) teflonised with 33 weight percent PTFE [14,24,25]. The thermoplastic elastomer such as styrene-ethylene / butyrene-styrene block copolymer (SEBS) has been used successfully as binding materials for MH electrodes [26]. 2-5 weight percent of SEBS gives the best discharge rate and capacity. SEBS has a rubber-like properties and is soluble in organic solvents allowing separation of alloy powder from a used electrode for recycling as well. In another method metal hydride alloy powder is mixed with cobalt and nickel powders and mechanically pressed alongwith a net of woven pure nickel wire to form an electrode strip [27]. This is similar to a process in which alloy powder was packed into foamed nickel by cold pressing [28].

Chapter 3

Fabrication of Ni-MH battery

3.1 The current collector

The current collector is a metallic strip or mesh and an important component of both the electrodes in Ni-MH batteries. This serves two purposes: (a) acts as a mechanical support and base for the active material, and (b) accepts current, resulting from reactions at numerous sites lying at the inner and outer surfaces of the electrodes.

Its selection is usually based upon the type of battery and the charging current requirements. The current collector should have the following characteristics :

- porous structure in which metallic particles can be attached with a binder,
- capacity to withstand the temperature rise (during charging and discharging) without compromising with mechanical properties,
- low electrical resistivity to lead to a minimum internal resistance,
- high corrosion resistance with regard to KOH solution, and

- chemically inert.

Nickel , stainless steel or nickel plated steel mesh is generally used for the electrodes. In the present case , we used a stainless steel mesh after thorough cleaning The steps involved are

(a) washing with hot distilled water,

(b) degreasing with 10% NaOH solution and repeating step(a),

(c) pickling with dil. H_2SO_4 and repeating step(a),

(d) drying in an oven and storage in a desiccator.

3.2 The electrolyte

The electrolyte is one of the three basic components of the cell. It acts like a bridge between two electrodes through which ions move. Obviously , it should have high electrolytic conductance and low reactivity with electrodes.

In Ni - MH battery KOH is used as an electrolyte. It is a white crystalline (rhombic) substance , molecular weight 56.10 , hygroscopic in nature and soluble in water. In the present case , potassium hydroxide pellets of 98% purity were dissolved in double distilled water to give a solution of 33% by weight. Its molality was 8.5. The viscosity (η) at 25°C, is estimated from the expression [3]

$$log\frac{\eta}{\eta_0} = A.c/(1 - B.c) \qquad (3\ 1)$$

where η_0 is the viscosity of pure water, c is the number of moles of KOH per litre of solution and A (= 0.0476),B (= 0.0199) are constants . This gives viscosity as 3.09 Centipoise and is quite reasonable. It may be noted that the viscosity of KOH

solution usually lies betwwen 1.5 and 5.0 Centipoise in the concentration range 20 - 45 % by weight for practical battery systems [3]. The dispersion capacity of KOH solution is determined by its diffusion coefficient (D), which is determined by

$$D = k \times \frac{T}{\eta} \tag{3.2}$$

where , k is the Boltzmann's constant ($= 1.38 \times 10^{-23}$ Joule / Kelvin). For our KOH solution diffusion coefficient takes a value of 1.32×10^{-19} m^2/s at 25°C.

3.3 The Separator

The separator has two functions to perform, namely physically separating the two electrodes to prevent short circuiting and holding of the electrolyte. So , the separator should be flexible , porous and have sufficient mechanical strength. It should not deteriorate in strong base and be able to withstand a temperature of 65°C In this work, we have utilised nylon cloth and glass wool for separating the two electrodes.

3.4 The nickel electrode

Traditionally , it consists of a sintered nickel substrate impregnated with active material $Ni(OH)_2$. The procedure involves complicated steps such as sintering in hydrogen atmosphere and electrochemical deposition of $Ni(OH)_2$ into the pores of the nickel substrate. This process results in nonuniform deposition and involves high cost. In our approach , $Ni(OH)_2$ powder was mixed with a conductive material and binder. The resulting paste was applied to a stainless steel grid and then pressed with a die, specially designed and constructed for the purpose. For the prepration of

$Ni(OH)_2$, 0.5 molar solution of $NiSO_4$ was mixed with one molar solution of NaOH (both in distilled water) to undergo a precepitation reaction

$$NiSO_4 + 2NaOH \rightarrow Na_2SO_4 + Ni(OH)_2 \downarrow \tag{3.3}$$

The precepitate was then filtered, washed with distilled water and filtered again . This process was repeated 20 times until the test for SO_4^{--} ion in washed out water came out to be negative. The purified precipitate was dried in an electric oven at 80°C (decomposition temperature of $Ni(OH)_2$ is 200°C) and analysed by X-ray powder diffraction method (see Section 4.1).

In the next step, we mixed $Ni(OH)_2$ powder with nickel and graphite separately and subjected to grinding in a ball mill for half an hour. These were then spread over stainless steel grid using a number of binders. Some of the methods employed were as under :

1. A paste of $Ni(OH)_2$ and graphite (in ratio of 5:1) in benzene was spread over a stainless steel mesh (7 cm x3.5 cm) pressed with the help of a die at a pressure of 12 tonnes. The resulting electrode was found to be conducting but adhesion was weak as during charging operation graphite and $Ni(OH)_2$ particles got detached from the grid structure.

2. Ni and $Ni(OH)_2$ were mixed with epoxy resin (arealdite) in different weight ratios (1, 2, 5 and 10%). It turned out that only above 5%, epoxy resin was able to bind successfully the metallic powder with the mesh to give a good homogeneous electrode structure. Alternatively, portland cement was tried in place of epoxy resin. The resulting structure was found to be porous in nature. However, in both the cases the resistence was very high. So, the electrodes

were considered to be not useful at all.

Since none of the above methods produced satisfactory results , we have opted for the nickel electrode used in the commercially available Ni - Cd rechargable batteries (AA size) in the present work

3.5 The metal hydride (MH) electrode

The MH electrode is the most important component of Ni-MH battery For this, $LaNi_5$ was ground in a ball mill (Fritsch, Germany) at 900 rpm for about 30 minutes, passed through a 100 mesh sieve and stored in a bottle containing acetone The powder is usually plasticised using P.T.F.E. . The technology is however not known Therefore, we tried an alternative method with silicone sealant as a binder. The reasons for selecting silicone sealant lie in its characteristic properties [29], viz it can survive chemical attack of 33% KOH , 30% H_2SO_4, phenol , H_2O_2 , O_3 , 10% muiatic acid, etc., and has high dielectrc strength (550 volts/mil), and low volume coefficient of thermal expansion ($\approx 9.3 \times 10^{-4}$ per degree celcius). Also on application it adheres to steel grid very well within 24 hours at room temperature and does not run off.

Using silicone sealant as a binder two types of MH electrodes have been fabricated, one using bare $LaNi_5$ powder as active material and other using electroless nickel coated $LaNi_5$ powder [30]. For this, $LaNi_5$ powder (6 g) was degreased in 20% NaOH solution. rinsed in water, etched for one minute in 50% volume / volume mixture of sulphuric acid (1 molar) and chromic acid (15 g/litre) and rinsed again in water. The powder was then immersed and held under suspension in an electroless nickel plating bath maintained at 90°C. The bath contained a solution

of nickel sulphate(7.5 g), sodium acetate (2.5 g) and sodium hypophosphite (2.5 g) in 250 ml of distilled water. After plating for 30 minutes, powder was rinsed in water and dried. As shown later, this process provides stability to $LaNi_5$ by reducing / controlling oxidation and hydrogen cracking effects. The MH electrode fabrication then involved rinsing of the steel grid in acetone and coating of silicone sealant and spreading of nickel coated $LaNi_5$ powder on both sides of the grid using a wooden paddle, and air drying for 24 hours.

3.6 Battery fabrication

The two electrodes with a separator sheet in between, were rolled together and put in a glass cylinder of outer diameter 1 8 cm and height 5.5 cm An another separator was introduced under the bottom metal hydride electrode so as not to allow that to come in contact with nickel electrode while being rolled. The open end of glass cylinder was sealed by a 2.5 mm thick nylon disc with arealdite . The nylon disc contained two holes of diameter 2mm each for taking out copper wire leades attached to the electrodes inside the battery. The outer end of the wires act as output terminal.

The details of various batteries fabricated are given in Table 3.1 .

Table 3.1 : Amounts of various components used in the fabrication of nickel metal hydride batteries number 1,2 and 3

No.	Component	Weight(g)		
		#1	#2	#3
1	$LaNi_5$ powder	5.110	4.462	4.793
2	Silicone sealant	1.795	1.567	1.723
3	Steel grid	2.482	2.262	2.308
4	$LaNi_5$ electrode	9.381	8.292	8.824
5	Ni electrode	5.989	5.982	5.986
	Total (4 + 5)	15.370	14.274	14.810

Chapter 4

Results and discussion

4.1 Phase(s) evaluation

The powder X-ray diffraction patterns of $LaNi_5$, $Ni(OH)_2$ and nickel coated $LaNi_5$ were recorded using Isodebyflex 2002 diffractometer with CuK_α radiation (λ = 1.5418 $\overset{o}{A}$) and a curve sensitive detector CPS 120 (ENEL, France). Fig. 4.1 shows the X-ray diffraction pattern of pure $LaNi_5$. It consists of six prominent peaks whose 2θ and relative intensity values are listed in Table 4.1 . The d-values correspond to a $CaCu_5$ type hexagonal structure having a = 5.016 $\overset{o}{A}$, c = 3.982 $\overset{o}{A}$ with c/a = 0.794 [31] . The Miller indices assigned to various reflections are also given in Table 4.1 .

The powder X-ray diffraction pattern of $Ni(OH)_2$ contains ten prominent peaks and is shown in Fig. 4.2 . The data extracted along with the Miller indices assigned are given in Table 4.2 . These suggest that $Ni(OH)_2$ prepared corresponds to a hexagonal structure having a = 3.126 $\overset{o}{A}$ and c= 4.605 $\overset{o}{A}$ [32].

Fig. 4.3 shows the X-ray diffraction pattern of nickel coated $LaNi_5$ powder.The

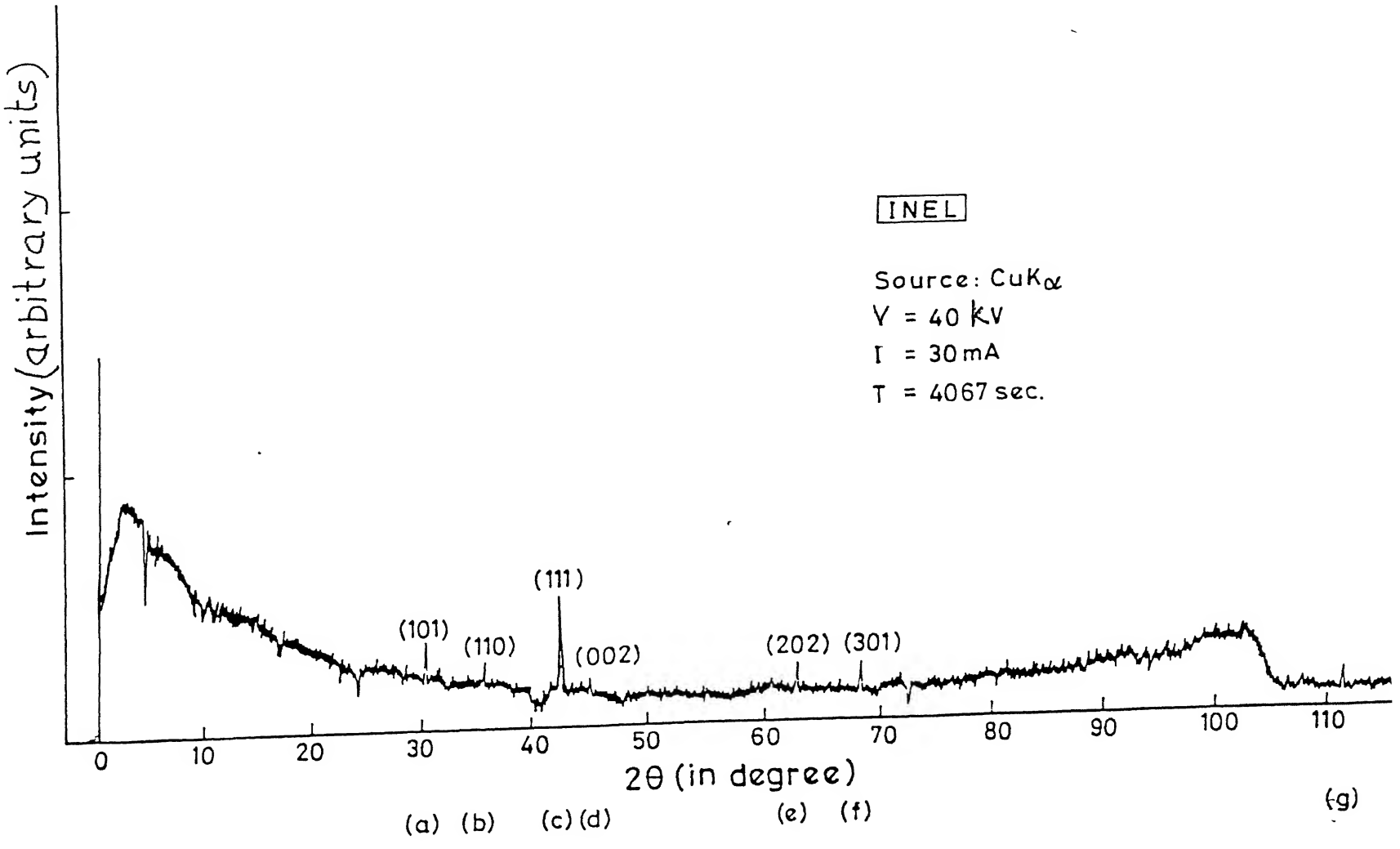

Fig. 4·1 X-ray diffraction pattern of $LaNi_5$

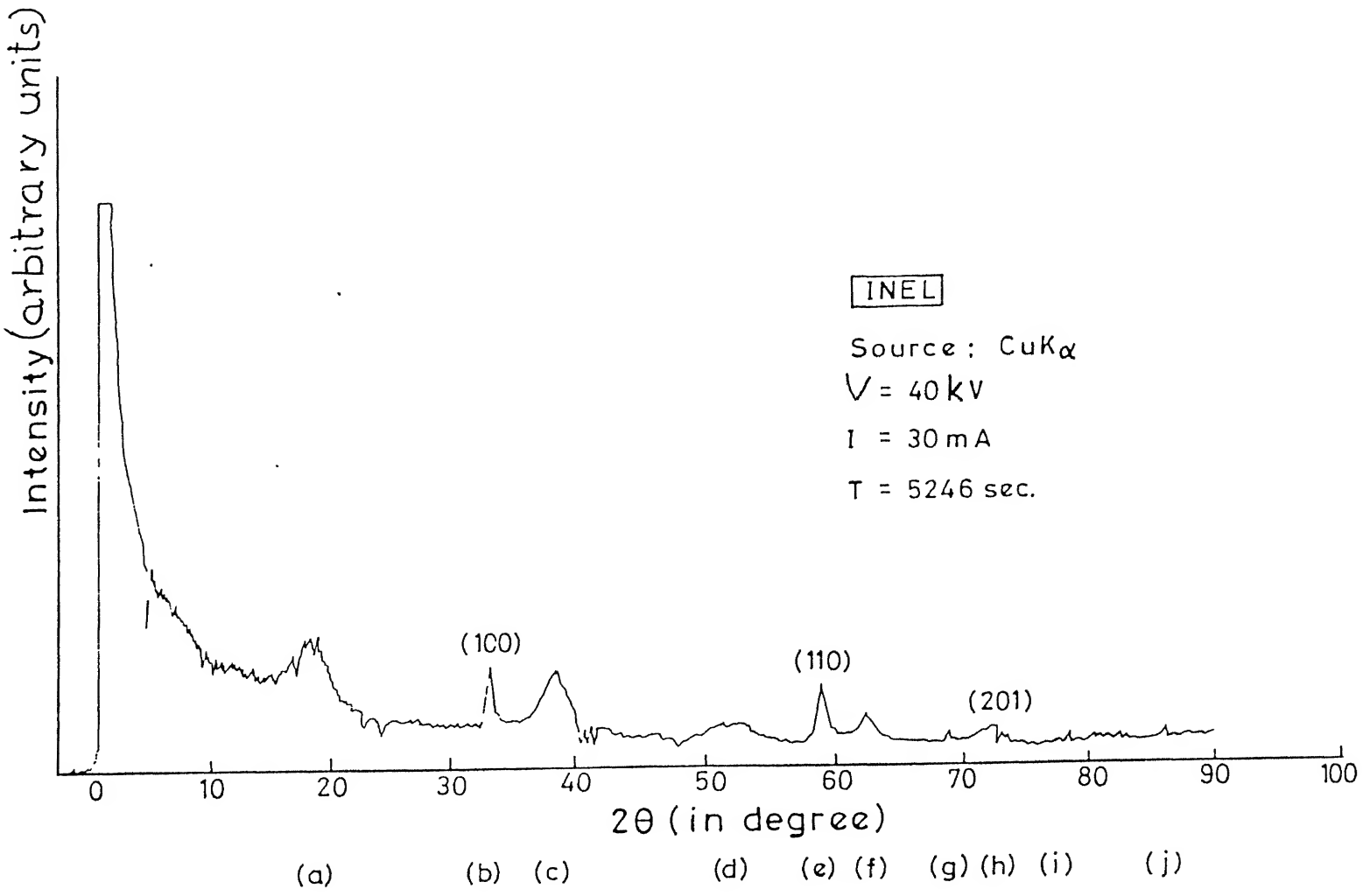

Fig. 4·2 X ray diffraction pattern of $Ni(OH)_2$

Table 4.1 : X-ray powder diffraction data of $LaNi_5$

No.	Peak	2θ (degree)	d_{hkl} (Å)	Relative intensity	d_{hkl} (Å) known [31]	Reflection hkl
1	a	30.5	2.92	38	2.926	101
2	b	35.9	2.50	13	2.503	110
3	c	42.5	2.12	100	2.120	111
4	d	45.2	2.00	23	1.988	002
5	e	62.8	1.47	29	1.467	202
6	f	68.3	1.37	50	1.360	301

Table 4.2 : X-ray powder diffraction data of $Ni(OH)_2$

No.	Peak	2θ (degree)	d_{hkl} (Å)	Relative intensity	d_{hkl} (Å) known [32]	Reflection hkl
1	a	19.0	4.60	22	4.605	001
2	b	33.2	2.70	100	2.707	100
3	c	38.0	2.40	36	-	-
4	d	53.0	1.73	2	1.754	102
5	e	59.0	1.56	80	1.563	110
6	f	62.0	1.49	5	1.480	111
7	g	69.0	1.36	3	1.335	103
8	h	72.5	1.30	34	1.299	201

2θ value and relative intensity of each reflection are given in Table 4.3 . It is indeed very complex. However, very careful examination of the d-values suggest the presence of $LaNi_5$ and nickel as main constituents with small traces of $Ni_3O_2(OH)_4$, γ - NiOOH and β - NiOOH [31-35].

4.2 The electrical characteristics

The electrical properties of Ni-MH battery fabricated are similar to a Ni-Cd battery, e g , the open circuit voltage is nearly same (1.3V). But, the charge acceptance is much faster in case of Ni-MH battery. It is expected too , as charge is stored in the form of hydride and movement of hydrogen is very fast. The main characteristics are discussed below:

The batteries were charged by a commercially available power supply giving 16 mA current at 2V output voltage. To determine state of overcharge / full charge , a common method is to constantly monitor the open circuit voltage. When there occurs a slight decrease or a constant value is reached the charging process is considered to be over and therefore stopped [1]. We , however, tried manual monitoring of the open circuit voltage. But, no voltage plateau was seen upto about four hours of charging. Also , in the process battery number 2 was exhausted. So these batteries were subjected to a flat charging at 2V with 15 mA current for 45 minutes.

The batteries were discharged through a resistance of 920 ohms using the electrical circuit shown in Fig.4.4 . The current and voltage were measured with a $4\frac{1}{2}$ digit panel current meter (HIL 2301) and a digital volt-ohm meter(HIL 2121),

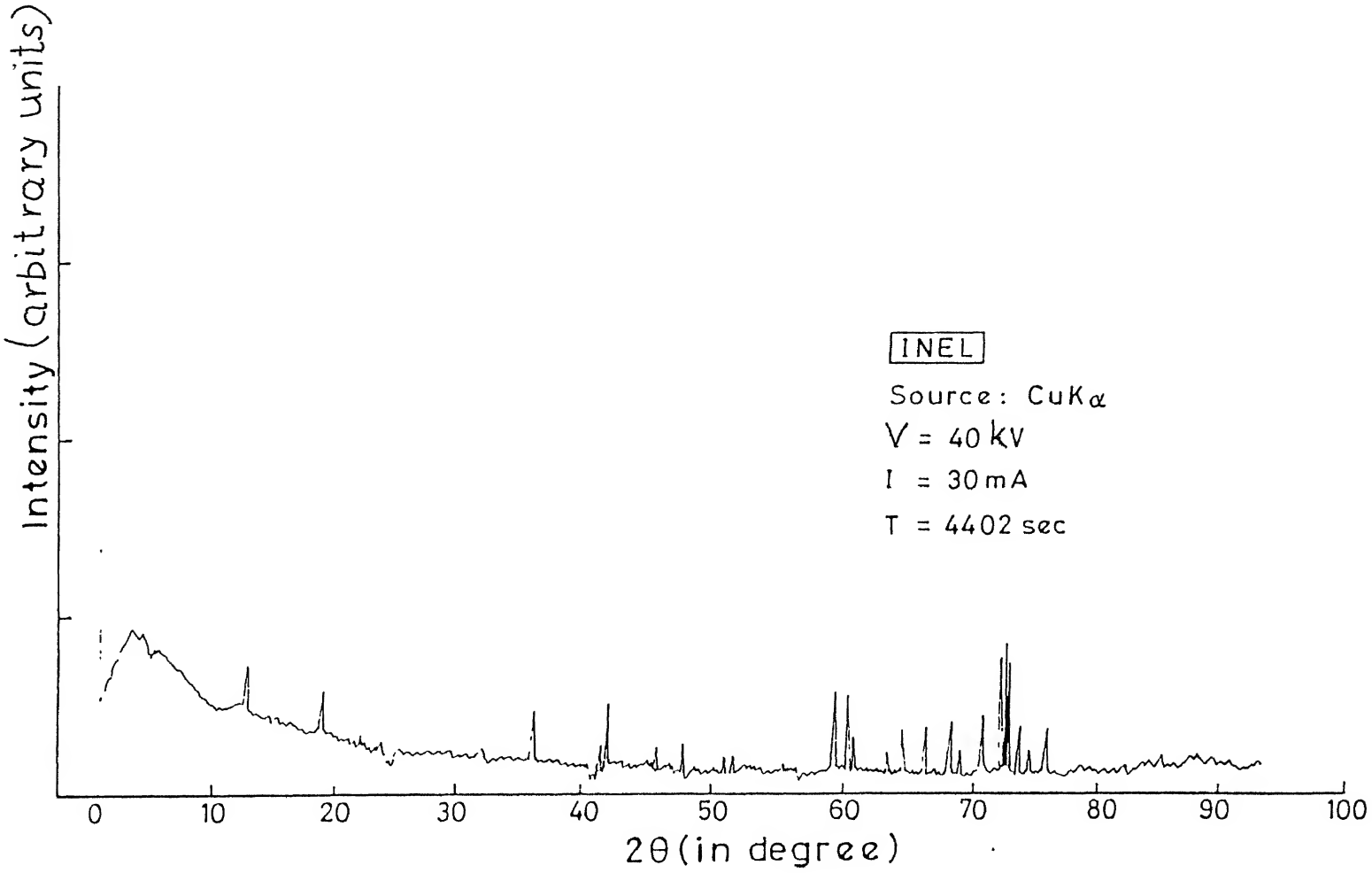

Fig. 43 X-ray diffraction pattern of Nickel coated $LaNi_5$

Table 4.3 : X-ray powder diffraction data of nickel coated $LaNi_5$

No.	2θ (degree)	d_{hkl} (Å)	Relative intensity
1	12.8	6.910	7.0
2	19.3	4.730	3.5
3	36.2	2.480	11.5
4	42.2	2.140	7.5
5	42.9	2.090	100.0
6	45.6	1.985	1.0
7	47.8	1.900	12.5
8	51.5	1.772	1.0
9	52.1	1.762	1.5
10	59.2	1.552	21.0
11	60.7	1.524	1.2
12	60.9	1.519	1.0
13	63.2	1.460	4.5
14	64.3	1.447	4.0
15	66.2	1.409	5.5
16	66.6	1.401	3.5
17	68.8	1.363	4.0
18	70.7	1.335	48.0
19	72.0	1.309	22.0
20	72.5	1.302	15.0
21	73.5	1.286	7.0
22	74.6	1.274	2.0
23	75.8	1.253	17.0
24	76.5	1.243	3.0

respectively. The current -time -voltage data are summarized in Tables 4.4, 4.5 and 4.6 for battery number 1,2, and 3 respectively. The power, average energy, internal resistance and energy density were calculated using the following relations [1].

$$power = mid\ point\ voltage \times\ midpoint\ discharge\ current \tag{4.1}$$

$$average\ energy = power \times time(seconds) \tag{4.2}$$

$$Internal\ resistance\ (r) = \frac{V}{i} - R_{external} \tag{4.3}$$

where V is in mV, i is in mA & $R_{external}$ is 920 ohms.

$$Energy\ density = \frac{E}{M} \tag{4.4}$$

where E is the total energy stored and defined as integral of power-time curve and M is the total weight of both the electrodes (i.e., metal hydride and nickel). Internal resistance and energy density figures are given in Table 4.9. The voltage, current and power profiles are shown in Fig. 4.5, 4.6 and 4.7, respectively. These clearly reveal that current and battery voltage drop similarly during discharge. The decrease in power ($\frac{V^2}{R}$) takes place more rapidly because of voltage exponent 2. The watthour efficiency can be estimated from

$$\eta_w = \frac{Watthours\ delivered\ on\ discharge}{Watthour\ needed\ to\ charge} \tag{4.5}$$

This gives η_w as $\approx$ 11-13% for all the batteries fabricated .

4.3 Effect of nickel encapsulation

As pointed out earlier , we initially fabricated Ni-MH batteries using bare $LaNi_5$ powder . As a consequence , these quickly lose the stored charge under

Figure 4.4: The discharging circuit

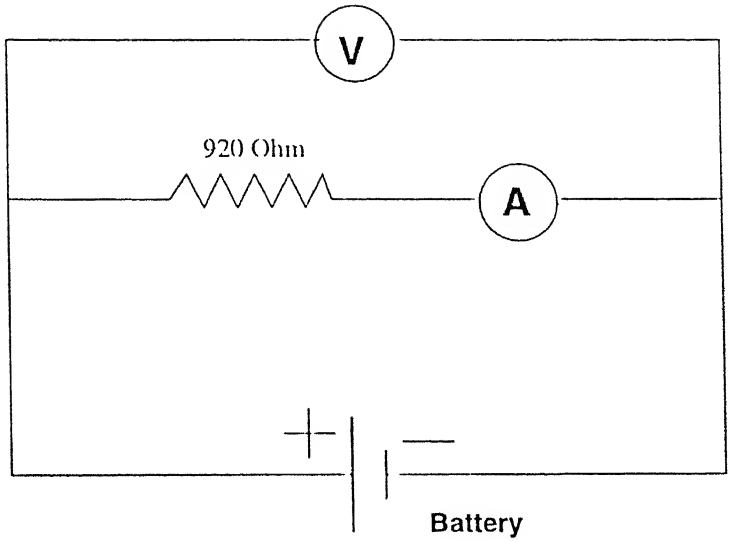

Figure 4.5: Voltage Profile

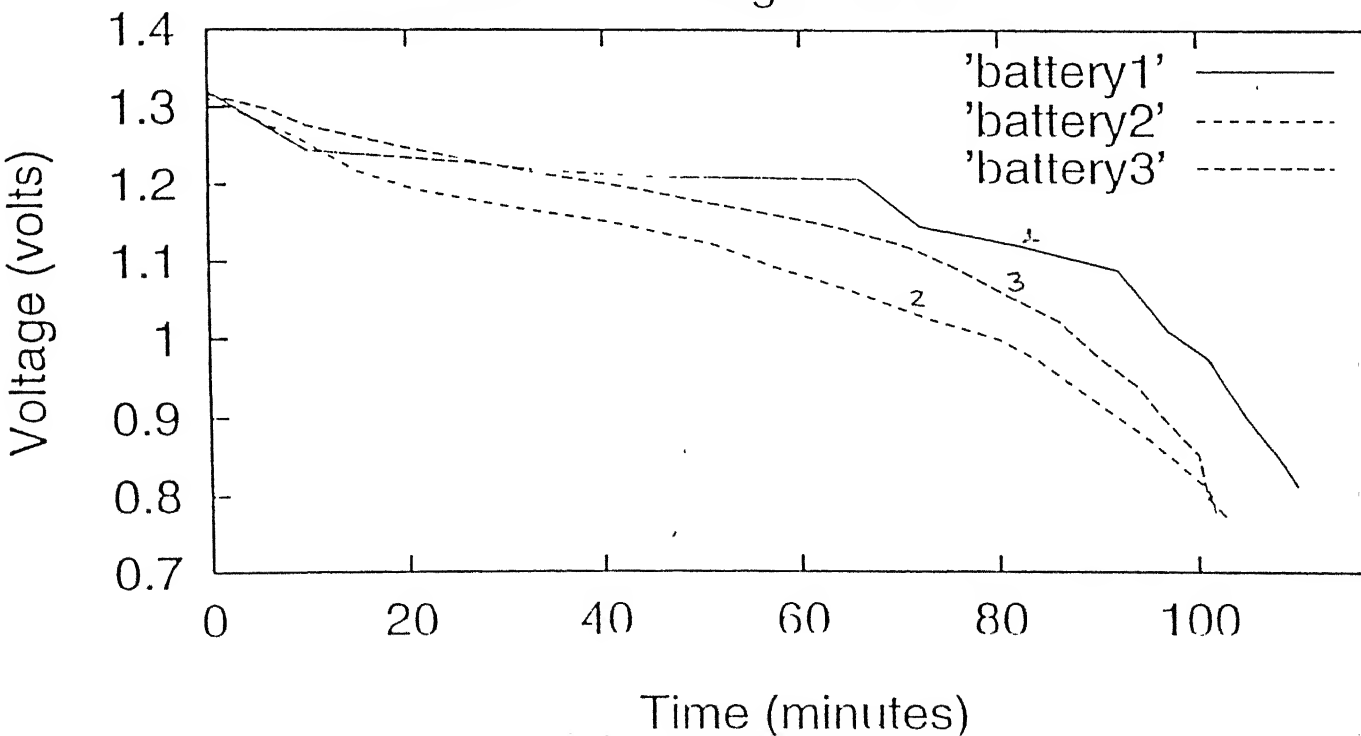

Figure 4.6 : Current profile

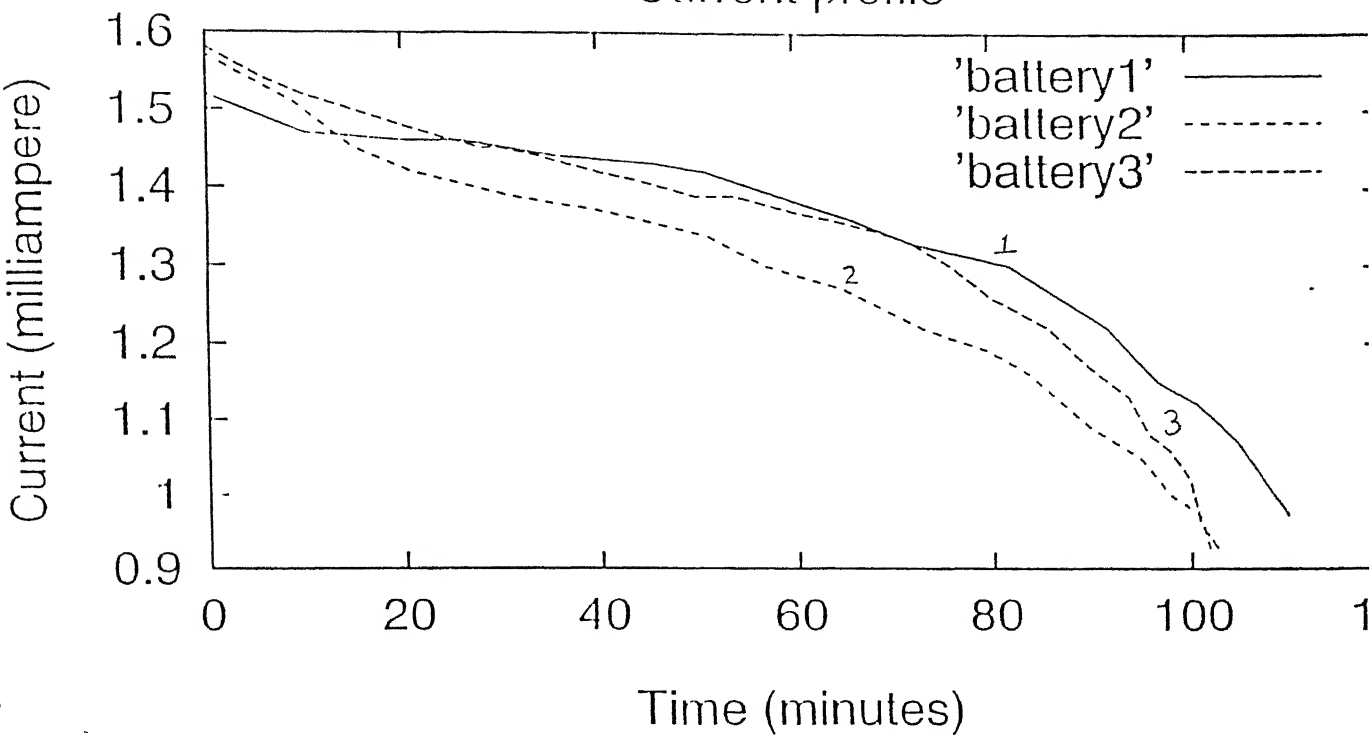

Figure 4.7 : Power profile

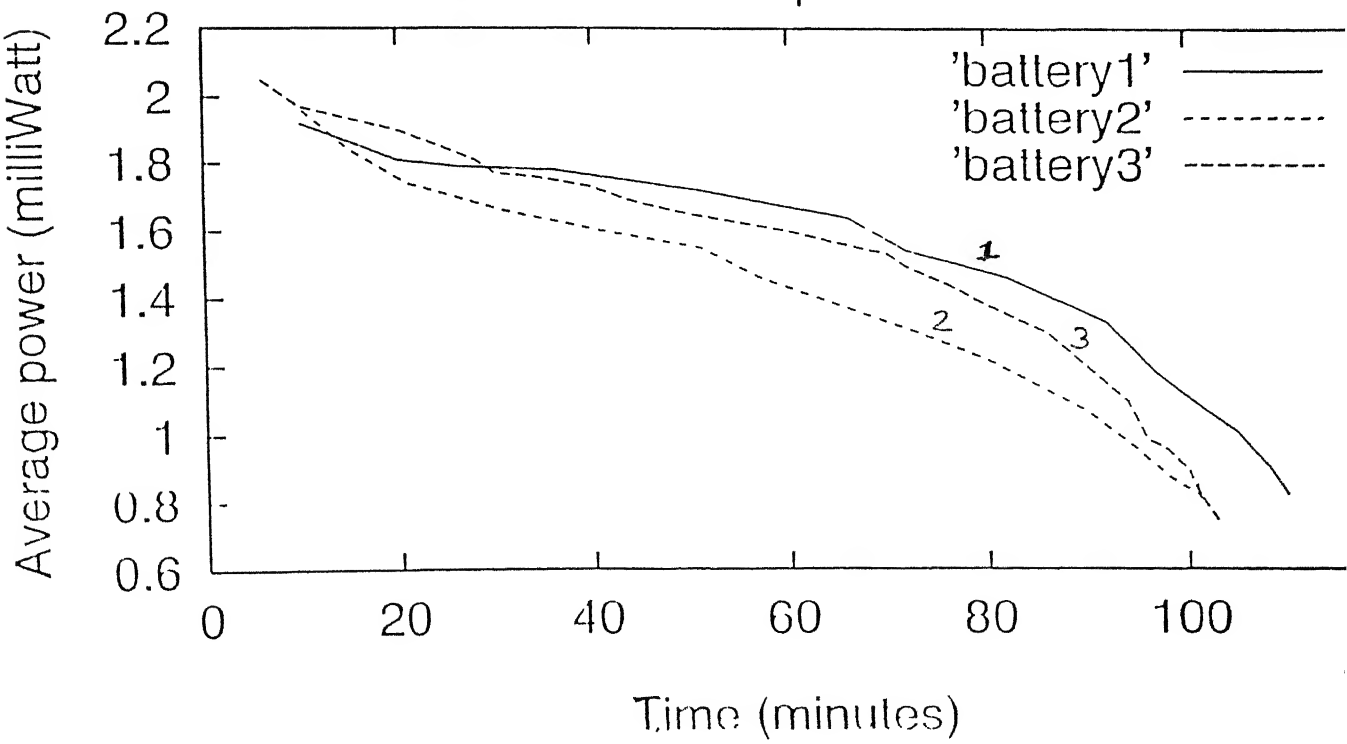

Table 4.4 : Discharge charateristics of nickel–metal hydride battery 1

No.	Time (Minutes)	Voltage (Volt)	Current (mA)	Average Power (mW)	Energy (mJ-s)
1	0	1.320	1.52	-	-
2	10	1.245	1.47	1.92	1149
3	20	1.236	1.46	1.81	1086
4	26	1.230	1.46	1.79	645
5	36	1.217	1.44	1.78	1068
6	46	1.210	1.43	1.74	1044
7	51	1.210	1.42	1.72	516
8	66	1.147	1.36	1.64	1476
9	72	1.122	1.33	1.54	554
10	82	1.090	1.30	1.46	876
11	92	1.012	1.22	1.33	798
12	97	0.978	1.15	1.18	354
13	101	0.941	1.12	1.09	196
14	105	0.899	1.07	1.01	242
15	108	0.851	1.01	0.91	164
16	110	0.814	0.97	0.82	98
				Total	10266

Table 4.5 : Discharge characteristics of nickel–metal hydride battery '2'

No.	Time (Minutes)	Voltage (Volt)	Current (mA)	Average Power (mW)	Energy (mJ-s)
1	0	1.312	1.57	-	-
2	9	1.262	1.51	1.98	1072
3	15	1.218	1.45	1.84	662
4	21	1.193	1.42	1.73	625
5	31	1.170	1.39	1.66	999
6	41	1.151	1.37	1.60	960
7	51	1.124	1.34	1.55	927
8	57	1.095	1.30	1.46	527
9	65	1.063	1.27	1.38	665
10	73	1.026	1.22	1.30	624
11	80	1.001	1.19	1.22	585
12	84	0.975	1.16	1.16	278
13	90	0.920	1.09	1.07	385
14	95	0.874	1.05	1.96	288
15	98	0.842	1.00	0.88	158
16	101	0.810	0.97	0.82	148
17	102	0.768	0.92	0.79	47
				Total	8950

Table 4.6 : Discharge characteristics of nickel–metal hydride battery '3'

No.	Time (Minutes)	Voltage (Volt)	Current (mA)	Average Power (mW)	Energy (mJ-s)
1	0	1.316	1.58	-	-
2	6	1.298	1.54	2.05	738
3	10	1.277	1.52	1.97	473
4	20	1.249	1.48	1.90	1140
5	28	1.229	1.45	1.81	869
6	30	1.223	1.45	1.77	212
7	34	1.214	1.44	1.76	422
8	40	1.202	1.42	1.72	621
9	44	1.193	1.41	1.69	406
10	50	1.178	1.39	1.65	594
11	54	1.169	1.39	1.63	391
12	60	1.155	1.37	1.60	576
13	64	1.142	1.36	1.57	377
14	70	1.124	1.34	1.53	551
15	72	1.114	1.33	1.49	179
16	76	1.090	1.30	1.44	346
17	80	1.062	1.26	1.38	331
18	86	1.024	1.22	1.29	466
19	90	0.980	1.17	1.20	288
20	94	0.942	1.13	1.10	265
21	96	0.909	1.08	0.99	119
22	98	0.880	1.06	0.96	115
23	100	0.854	1.02	0.90	108
24	101	0.798	0.96	0.82	50
25	103	0.771	0.92	0.73	88
				Total	9725

Table 4.7 : Discharge charateristics of nickel–metal hydride battery '1' after 25 cycles

No.	Time (Minutes)	Voltage (Volt)	Current (mA)	Average Power (mW)	Energy (mJ-s)
1	0	1.320	1.52	-	-
2	10	1.240	1.47	1.91	1146
3	20	1.231	1.45	1.80	1080
4	30	1.219	1.44	1.77	1062
5	40	1.212	1.43	1.74	1044
6	50	1.207	1.42	1.72	1032
7	60	1.163	1.37	1.66	996
8	70	1.121	1.32	1.55	930
9	80	1.079	1.28	1.43	858
10	85	1.048	1.25	1.34	403
11	90	1.009	1.21	1.26	369
12	95	0.973	1.14	1.16	379
13	98	0.913	1.09	1.05	189
14	101	0.874	1.04	1.95	171
15	103	0.845	1.99	0.87	104
16	105	0.816	0.98	0.81	91
				Total	9854

Table 4.8 : Discharge characteristics of nickel–metal hydride battery '3' after 25 cycles

No.	Time (Minutes)	Voltage (Volt)	Current (mA)	Average Power (mW)	Energy (mJ-s)
1	0	1.320	1.58	-	-
2	5	1.303	1.55	2.05	738
3	10	1.276	1.52	1.97	472
4	20	1.247	1.48	1.89	1134
5	30	1.221	1.45	1.80	1080
6	35	1.210	1.44	1.75	526
7	40	1.200	1.42	1.72	516
8	45	1.197	1.41	1.69	507
9	50	1.175	1.39	1.65	495
10	55	1.157	1.37	1.61	483
11	60	1.153	1.37	1.58	474
12	65	1.136	1.35	1.55	467
13	70	1.121	1.34	1.52	456
14	75	1.091	1.30	1.45	437
15	80	1.058	1.26	1.37	413
16	85	1.026	1.22	1.29	387
17	90	1.980	1.17	1.19	359
18	93	1.949	1.13	1.10	199
19	96	0.899	1.07	1.00	180
20	99	0.848	0.01	0.89	161
21	101	0.810	0.99	0.82	99
22	103	0.749	0.90	0.73	88
				Total	9671

Table 4.9 : Variation of open circuit voltge of nickel-metal hydride batteries

Number of days	Open circuit voltage (Volt)	
	Battery No. 1	Battery No. 3
-	1.30	1.300
2	0.3	1.298
60	0.1	0.978

Table 4.10 : Characteristic parameters of nickel-metal hydride batteries

Parameter	Battery No. 1	Battery No. 2	Battery No. 3
Internal resistance (ohm)	75	80	73
Energy density (J-s/kg)	667	626	656

Table 4.11 : Effect of Ni-encapsulation on the stability, open circuit voltage and capacity of nickel-metal hydride batteries.

Parameter	Battery No. 1	Battery No. 3
Percentage drop in open circuit voltage after 60 days	92.30	24.80
Stability factor(s) after 25 cycles	0.96	0.99
Average drop per cycle in capacity after 25 cycles	1.6×10^{-3}	0.4×10^{-3}

open circuit condition (Table 4.10) due to poor stability. The battery '1' was subjected to 25 charge-discharge cycles to determine its functional stability. The characteristics after 25 cycles are given in Table 4.7 . It can be noticed that the total energy stored in 25th cycle is less than that stored in the first cycle. Obviously, there is a clear degradation in capacity of battery '1' during the charge-discharge cycles As mentioned earlier, battery '2' was exhausted during the first few charging cycles only.

The charge storage capacity and its retention upon subsequent electrochemical cycling is yet another important parameter for a hydride forming electrode. Usually the storage capacity decreases with each cycle [7], a feature prevailing in the present Ni-MH battery as well. The stability factor S(n) can be defined as

$$S(n) = \frac{C_t(n)}{C_t(0)} \tag{4.6}$$

where $C_t(n)$ refers to the storage capacity after n cycles . Obviously , S(n) gives the fraction of the initial storage capacity at any instant . The decrease of $C_t(n)$ or stability factor S(n) is associated with the degradation of $LaNi_5$ itself. In fact, the hydrogen absorption / desorption process leads to reduction in particle size due to considerable volume expantion ($\approx 25\%$) and the associated stress / strain causing cracking. Also, only a partial release of hydrogen occu rs during the discharge cycle. Besides, surface oxidation of active $LaNi_5$ particles takes place in alkali media via an irreversible first order reaction of the type

$$LaNi_5 + 3H_2O \rightarrow La(OH)_3 + 5Ni + \frac{3}{2}H_2 \tag{4.7}$$

The presence of the above reaction products have been detected by XRD earlier [36] and are assumed to cover the underlying active $LaNi_5$. Thus , there is an effective

coverage and simultaneous reduction in amount of the active material with each cycle . Obviously , storage capacity has to decrease and can be considered to be proportional to the amount of active material left *Notten et. al.*[35] have derived an expression for $C_t(n)$ as

$$[C_t(n)]^{\frac{1}{3}} = [C_t(0)]^{\frac{1}{3}}\{1 - \frac{A_0.K_{ox}.a_{H_2O}.M_{LaNi_5}.t}{3}\} \tag{4.8}$$

where A_o is the specific surface area of starting material , K_{ox} is the oxidation rate constant , a_{H_2O} is the activity of water , M_{LaNi_5} is the molecular weight of $LaNi_5$ and t is the elasped time For retention of the initial storage capacity, it is necessary that the A_o and K_{ox} both be small . While the former relates inversely to the particle size, the later depends on the oxidation charateristics of the active material itself.

In order to overcome degradation problems, we fabricated battery '3' with metal-hydride electrode made of electroless nickel coated $LaNi_5$ powder and subjected to same kind of tests. The results were quite encouraging as improvements occurred in both the shelf life (i.e., low self discharge) and capacity loss , as indicated in Tables 4.8 and 4.9. Yet another parameter giving average fractional drop per cycle in capacity can be approximated by considering linear relationship as

$$S'(n) = \frac{1 - S(n)}{n} = \frac{C_t(0) - C_t(n)}{n.C_t(0)} \tag{4.9}$$

Similarly, fractional drop in open circuit voltage after time t can be given by

$$[\frac{dV}{V}]_t = \frac{V_0 - V_t}{V_0} \tag{4.10}$$

Where V_0 is the initial open circuit voltage and V_t is the voltage after maintaining the open circuit condition for time t. While S'(n) is evaluated after 25 cycles, $(\frac{dV}{V})_t$ is determined after 60 days of self discharge. The results are presented in Table 4.11.

These clearly show improvement in characteristics (e.g., much higher stability) for nickel coated MH electrode battery.

This can be understood by effective decrease of the oxidation rate constant K_{ox} as well as the controlled passage of hydrogen through nickel coated layer to $LaNi_5$ causing less damage and less effect on the particle size. Nickel coating also acts as a local current collector to facilitate the discharge transfer reaction on the alloy surface. Alternatively one has to develop another hydrogen storage compound of lower K_{ox}, as attempted by others [37-40]. As pointed earlier, battery self discharge is due to hydride stability under open circuit condition.The microencapsulation results in protection of alloy against strongly oxidising environment inside the battery by providing a barrier of stable nickel layer.

Conclusions

1. Nickel - metal hydride rechargeable cylindrical battery (size 'AA') has been successfully fabricated using nickel coated $LaNi_5$ as active material with silicone sealent as binder (for the negative electrode),$Ni(OH)_2$ electrode, 8.5 molal solution of KOH as an electrolyte , and a combination of nylone cloth and glass wool as separator. Their typical open circuit voltage is 1.3 V with energy density equal to approximately 656 J-s/kg .

2. Silicone sealant has proved to be a good binding material and can replace P.T.F.E. in the fabrication of MH electrode.

3. For charging / discharging cycle, it is necessary to have a totally sealed rather than vented construction for the battery .

4. The quantity of electolyte should be just sufficient to wet the separator as otherwise excessive gas evolution occurs - adversely affecting the seal.

5. Microencapsulation of $LaNi_5$ powder with electroless nickel coating was found to be very effective in improving the stability and performance of MH electrode. It not only prevents oxidation of $LaNi_5$ but also acts as local current collector causing in improvement in the recycling capacity and the reduction in the self discharge effect of the Ni-MH battery.

Scope for further work

In the present work many interesting pitfalls were encountered. Some of these requiring further investigations are :

(a) Development of $Ni(OH)_2$ electrode.

(b) The battery (cell) fabricated exhibit high internal resistance. So better contact between support grid and metal hydride powder is necessary. Also, modifications of KOH electrolyte is to be examined by addition of better conducting LiOH.

(c) Encapsulated LaNi5 powder particles contain Phosphorous/Phosphite ions due to the presence of sodium hypophosphite in the plating bath. The stability achieved in MH electrode needs to be evaluated as a function of phosphorous content.

(d) The full charge state of Ni-MH batteries could not be determined due to step wise rather than continuous monitoring of open circuit voltage . Thus evaluation of storage capacity should be done after insuring full charged condition.

Appendix

1. Important electrochemical constants / terms :

   - Faraday constant = 96,487 C
   - Ampere hour (Ah) = Current (A) * time (h)
   - 1 electron flow per second = 4.44 * 10^{-23} Ah
   - Capacity (Ah/g) = 26.8 / (Equivalent weight of active material)

2. Theoretical voltage and capacity of major battery systems [1] :

Battery	Anode	Cathode	Capacity		
			V	g/Ah	Ah/kg
Lead - acid	Pb	PbO_2	2.1	8.32	120
Edison	Fe	NiOOH	1.4	4.46	224
Nickel - Cadmium	Cd	NiOOH	1.35	5.52	181
Nickel - Hydrogen	H_2	NiOOH	1.5	3.46	289
Nickel - metal hydride	MH	NiOOH	1.35	6.50	206
Silver - cadmium	Cd	AgO	1.40	4.41	227
Sodium - sulfur	Na	S	2.1	2.65	377
H_2/O_2 fuel cell	H_2	O_2	1.23	0.336	2975

3. Technical details about important Ni-Cd cylindrical sealed cells

Size	Rated Capacity (mAh at 25°C)	Overcharge rate (mA)		Size (mm)	
		maximum	minimum	diameter	height
$\frac{1}{3}$ AA	100	10	5	15.0	17.9
$\frac{1}{3}$ A	150	15	8	16.7	16.7
$\frac{1}{2}$ AA	250	25	13	15.0	32.5
$\frac{2}{3}$ A_F	400	40	20	17.1	28.5
AA	450	45	23	14.6	50.0
$\frac{1}{2}$ C_S	550	55	28	23.0	26.6
A	600	60	30	16.7	49.9
C_S	1000	100	50	23.0	41.8
$\frac{3}{5}$ C	1000	100	50	26.3	30.1
$\frac{2}{3}$ C	1000	110	55	26.3	33.1
C	1500	150	75	26.3	47.2
$\frac{1}{2}$ D	2000	200	100	33 1	37.2
D	3500	350	175	33.1	59.6
F	5600	560	280	33.1	88.6

Ni-Cd battery application engineering handbook, General electric company, USA

Diameter includes 0.8 mm usual allowance for insulating sleeve

References

[1] David Linden, "*Handbook of batteries*" second edition, McGraw Hill, NewYork, 1996

[2] S. U. Falk and A. J. Salkind, "*Alkaline Storage Batteries*" first edition, John Willey and sons, NewYork , 1969.

[3] L. F. Martin , "*Storage batteries and rechargable cell technology*" first edition, Noyesdata Corporation, London, 1985.

[4] G. Wranglen , "*An introduction to corrosion and protection of metals*", Chapman and Hall, London, 1985.

[5] Raj Narayan , "*An introduction to metallic corrosion and ites prevention*", Oxford and IBH publishing company, New Delhi, 1983.

[6] Sanjeev Saxena, *Hydrogen absorption studies of* $(Fe_{0.9}M_{0.1})Ti$, $(Fe_{0.8}Ni_{0.2})Ti$ *and* $LaNi_5$, M. Tech. Thesis, IIT Kanpur, 1986.

[7] P. H. Notten, in *Interstitial intermetallic alloys*, F.Grandjen, Long G. J. and Busdow K. H. J. (editors), Kluwer, Dordreeht , 1995, P.151.

[8] A Verma, *Study of mischmetal intermetallics for Hydrogen storage*, M. Tech. Thesis, IIT Kanpur, 1984.

[9] O. G. Westlake, C. B. Sattertuwate and J. H. Weaver in *Physics Today*, Nov.1978, p. 320 .

[10] A. Lasia, D. Gregoire, *J. Electrochem. Soc.*, 142 p. 3393, 1995.

[11] M Ohitami, H¿ Yufu, K. Takashima, S. Tsuji and Y. Matsumaru, *J. Electrochem. Soc.*, 136, p.1590, 1989 .

[12] H Y. Chang, L. Dan Z. Wenhua, L. W. Hua, H. Z. Long, M. Kopezyk and W. Grazyna in, *New promising electrochemical systems for rechargable batteries*, V. Barsukov and F. Beck (editors), Kluwer, Dordreeht, 1996, p 247,

[13] R.Rani, S.Gupta, Jitendra Kumar, K. N. Rai, in *Proc. World Hydrogen energy Conf.(iv) Pergamon*, 3, p. 1245, 1982 .

[14] B. R. Babu, P. Periasamy and C. Chakkarovarty, *Bulletin of Electrochemistry*,p. 371, May 1993 .

[15] K.C. Ho, and J. Jorne, *J. Electrochem. Soc.*, 137, p. 144,1990 .

[16] H.H. Law and J. Sapjeta, *J. Electrochem. Soc.*,136, p. 1603,1989 .

[17] O. Fcherer, S. Riekf, C. Schmitz, B. Willer and M. Wollny, *Int. J. Hydrogen Energy*, 19, p. 34, 1994 .

[18] M. P. Sridhar kumar, W. Zhang, K. Petrov, A.A. Rostami and S. Srinivasan, *J. Electrochem. Soc.* , 142, p.3424, 1995 .

[19] T. Sakai, H. Miyamura, N.Kuriyama, A. kato , K. Oguro and H.Ishikawa, *J. Electrochem. Soc.*, 137, p. 705, 1990 .

[20] G D. Adzic, J.R. Johnson, J.J.reilly, J. Mcbreen, S. Mukherjee, M. P. Sridher Kumar, *J. Electrochem. soc.* 142, p. 3429, 1995 .

[21] C Iwahura, M. Matsuoka and T. Kohno, *J Electrochem. Soc.*, 141, p. 2306, 1994.

[22] T Ikeya, K. Kumai and T Iwahori, *J. Electrochem. Soc.* , 140, p.1062, 1993 .

[23] M. Ciiureahu, J O. Stromolsen, D. H. ryan, P. Rudkowski, G. Rudkowska and B. Bondoc, *J. Electrochem. Soc.* 141, p. 3291, 1994 .

[24] K. Petrov, A.A. Rostami, A. Visintin and S. Srinivasan, *J. Electrochem. Soc.*, 141 p. 1747, 1994 .

[25] C. Jun. and Z. Yunshi, *Int. J. Hydrogen energy*, 20, p. 235,1995 .

[26] T.Hara,N. Yasuda, T. Takeuchi, T. Sakai, A. Vichiyama, H. Miyamura, N. Kuriyama and H. Ishikawa, *J. Electrochem. Soc.*, 140, p. 2450, 1993 .

[27] Z.Ye, T. Sakai, D. Noreus, E. Rosen and E. Baring, *J. Electrochem. Soc.*, 142, p 4045, 1995 .

[28] T Sakai, T. Iwaki, Z. Ye, O. Noreus and O. Lindstrrom, *J. Electrochem. Soc.*, 142, p 1995.

[29] Application manual, *Silastic 732RTV adhesive/sealant*, DOW CORNING; U S.A

[30] R. K Kaul, *Preparation of composite powders by electroless plating*, M. Tech. Thesis, IIT Kanpur 1977 .

[31] *Powder diffraction file*, 17-126 .

[32] *Powder diffraction file*, 14-117.

[33] *Powder diffraction file*, 4-0850 .

[34] *Powder diffraction file*, 22-444 .

[35] *Powder diffraction file*, 6-0075

[36] P. H. L. Notten, J. L. C. Daams and R. E. F. Einerhand, *Physical Chem.*,19, p. 656, 1992

[37] J.J.G. Willems, *Philips J. Res. Suppl.*,39,p.1, 1984

[38] J.R.G.C.M. Vanbeek, J.J.G. Willems and H.C. Donkesloot, in *Proc. 14, Int, Power Sources Symp.*, Brighton, L. C. Pearce (editor), Power sources, 10,p. 317,1985

[39] J.J.G. Willems and K.H. bushow, *J. less common metals*, 13, p. 129, 1987

[40] Y Osumi, H. Susuki, A. Kato and K.Oguro, *J. Less common metals*, 39, p.287, 1983.